THE JOURNAL OF PHYSICAL CHEMISTRY A
A JOURNAL OF THE AMERICAN CHEMICAL SOCIETY

ACS AUTHORCHOICE

pubs.acs.org/JPCA

Article

Photolysis Production and Spectroscopic Investigation of the Highest Vibrational States in H_2 ($X^1\Sigma_g^+$ v = 13, 14)

Published as part of The Journal of Physical Chemistry virtual special issue "Cheuk-Yiu Ng Festschrift".

K.-F. Lai, M. Beyer, E. J. Salumbides, and W. Ubachs*

Cite This: *J. Phys. Chem. A* 2021, 125, 1221−1228

Read Online

ACCESS | Metrics & More | Article Recommendations

ABSTRACT: Rovibrational quantum states in the $X^1\Sigma_g^+$ electronic ground state of H_2 are prepared in the v = 13 vibrational level up to its highest bound rotational level J = 7, and in the highest bound vibrational level v = 14 (for J = 1) by two-photon photolysis of H_2S. These states are laser-excited in a subsequent two-photon scheme into $F^1\Sigma_g^+$ outer well states, where the assignment of the highest (v,J) states is derived from a comparison of experimentally known levels in $F^1\Sigma_g^+$, combined with *ab initio* calculations of $X^1\Sigma_g^+$ levels. The assignments are further verified by excitation of $F^1\Sigma_g^+$ population into autoionizing continuum resonances, which are compared with multichannel quantum defect calculations. Precision spectroscopic measurements of the F-X intervals form a test for the *ab initio* calculations of ground state levels at high vibrational quantum numbers and large internuclear separations, for which agreement is found.

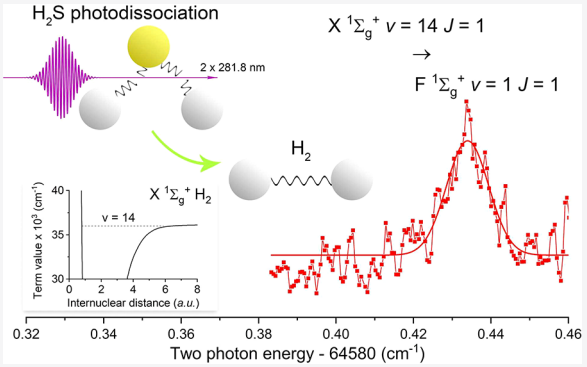

I. INTRODUCTION

The hydrogen molecule has been the benchmark species of molecular spectroscopy since the first analysis of its dipole-allowed absorption spectrum, now over a century ago.[1] Over decades, further detailed experiments on the electronic spectrum were performed,[2−4] while also the measurements of forbidden vibrational transitions were explored.[5] Alongside, and stimulated by experimental observations, the quantum theory of the ground state of the smallest neutral molecule was developed with major contributions from James and Coolidge,[6] Kołos and Wolniewicz,[7] and Wolniewicz.[8] The excited states and the strong effects of nonadiabatic interactions were investigated by Dressler and co-workers.[9] The theoretical program of refined calculations of the ground state structure was further extended by Pachucki and co-workers including effects of nonadiabatic, relativistic, and quantum-electrodynamical (QED) effects,[10,11] which has now produced an online program (H2SPECTRE[12]) to compute level energies for all rovibrational states of the hydrogen isotopomers.[13]

Spectroscopic studies of molecular hydrogen have included the behavior at long internuclear separation. Characteristic for the level structure of H_2 is the occurrence of double-well potential energy curves for excited states, induced by strong nonadiabatic interactions in this light molecule. In the manifold of g-symmetry the lowest of these is the $EF^1\Sigma_g^+$ state, for which the outer well was investigated,[14,15] followed by the $GK^1\Sigma_g^+$ and $H\bar{H}^1\Sigma_g^+$ states.[16,17] Similarly double-well states of $^1\Pi_u$ symmetry[18,19] and of $^1\Sigma_u^+$ symmetry were investigated.[20,21] These studies on long-range effects in the hydrogen molecule were extended to higher energies, leading to observation of exotic phenomena as ion-pair or heavy Rydberg states,[22] quasi-bound states,[23] and shape resonances[24] in the molecular ion.

Various approaches have been followed to investigate H_2 in vibrationally excited states of the $X^1\Sigma_g^+$ electronic ground state, also exhibiting wave function density at large internuclear separation. Moderately excited v-levels were probed in chemical reaction dynamical studies,[25,26] with hot filaments.[27,28] and in a high voltage discharge.[15] Instead of producing the vibrationally excited states over a wide population distribution, Zare and co-workers proposed Stark-induced Raman passage to prepare a single desired state of H_2[29] and recently showed controlled transfer of large population to v = 7, J = 0.[30]

Steadman and Baer investigated the production of vibrationally excited states via the two-photon ultraviolet photolysis

Received: December 14, 2020
Published: January 27, 2021

of H_2S.[31] The results of this one-laser experiment was further investigated in two-laser[32] and three-laser experiments[33,34] leading to accurate level energies and test of quantum electrodynamics in $X^1\Sigma_g^+$, v = 11−12. Alternatively, the UV-photolysis of formaldehyde (H_2CO) was used for the production and investigation of H_2 in $X^1\Sigma_g^+$, v = 3−9.[35] In these studies the wave function density at large internuclear separation, as occurring in high-v states, was probed via two-photon excitation to the $F^1\Sigma_g^+$ outer well state.

In the present study, the two-photon UV photolysis production of vibrationally excited H_2 from H_2S is extended by increasing the photon energy of the dissociation laser. By this means the dissociation channel for producing $X^1\Sigma_g^+$, v = 13−14 becomes energetically possible. These highly excited vibrations are interrogated with Doppler-free 2 + 1′ resonance multiphoton ionization (REMPI) spectroscopy in a three-laser scheme. Precision measurements probing $F^1\Sigma_g^+$, v = 0,1 outer well levels allow for testing high-accuracy quantum chemical calculations of H_2 in the regime of large internuclear separation.

II. EXPERIMENT

The experimental layout, shown in Figure 1, is similar to the one used in previous studies probing H_2 in v = 11, 12.[33,34]

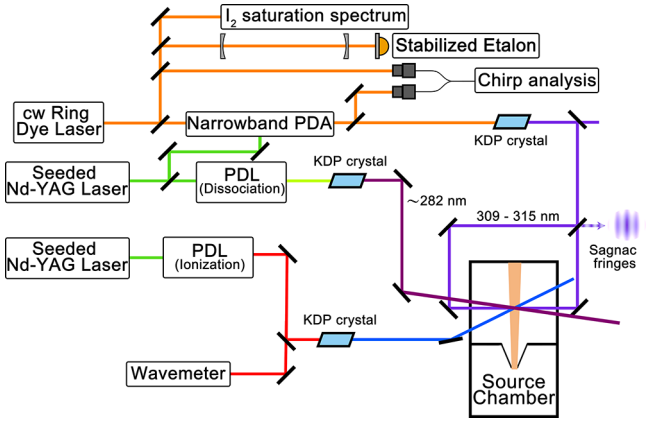

Figure 1. Schematic layout of the experimental setup including the three UV-lasers, the calibration units, and the vacuum chambers. For details, see text.

Three ultraviolet (UV) pulsed laser systems are involved for producing the highest vibrational levels in H_2 from H_2S photolysis and detection by 2 + 1′ REMPI. The two-photon UV-photolysis proceeds via the path:

$$H_2S \xrightarrow{2h\nu} S(^1D_2) + H_2(X^1\Sigma_g^+,\ v = 8 - 14) \quad (1)$$

The wavelength of the dissociation laser is set at 281.8 nm, as opposed to 291 nm in the previous studies, since the energy required for complete dissociation of H_2S to form an $S(^1D_2)$ atom and two $H(^2S)$ atoms is about 69935(25) cm^{-1}.[36] The two-photon energy for 281.8 nm dissociation lies about 1000 cm^{-1} above this limit, which is needed to produce H_2 in the highest vibrational levels close to the dissociation limit. Focused UV-pulses at energies of 4.5 mJ are used for the photolysis step.

Vibrationally excited H_2 is interrogated by a narrowband pulsed-dye-amplifier (PDA) system via probing of the $F^1\Sigma_g^+$−$X^1\Sigma_g^+$ two-photon transition. The PDA is seeded by the output of a continuous wave (cw) ring-dye laser and its pulsed output is frequency doubled in a KDP crystal to deliver wavelength tunable UV pulses in the range 309−315 nm. The bandwidth of this PDA is about 150 MHz in the UV. The UV pulse is split and configured into a counter-propagating geometry, shown in Figure 1, and adjusted into a Sagnac interferometric alignment for reducing possible Doppler shifts.[37] The absolute frequency of the cw-seed light is calibrated by measurement of hyperfine-resolved saturation spectra of I_2 for reference, where markers of a stabilized etalon are used for interpolation. The chirp of the pulses of the PDA is analyzed and corrected for following known procedures.[38]

The third UV pulse, obtained from another frequency-doubled pulsed-dye-laser (LIOP-TEC), excites population in the $F^1\Sigma_g^+$-state into the H_2^+ ionization continuum for detection. The autoionization spectra from F-states are recorded by scanning through 315−320 nm. The frequency of PDL output is calibrated with a HighFinesse WSU-30 (Toptica) wavemeter. In the case when precision measurements on the F-X transitions are performed, the third UV-laser is set on a strong autoionization resonance for signal optimization. Figure 2 illustrates the level structure of the H_2 molecule and the various excitation steps induced in the three-laser scheme.

All three UV beams are focused to a few tens of μm and are spatially overlapped with the H_2S effusive molecular beam. The PDA-spectroscopy laser is optically delayed by 10 ns from the dissociation laser, which is pumped by the same Nd:YAG pump laser. This is to avoid an ac-Stark shift induced by the

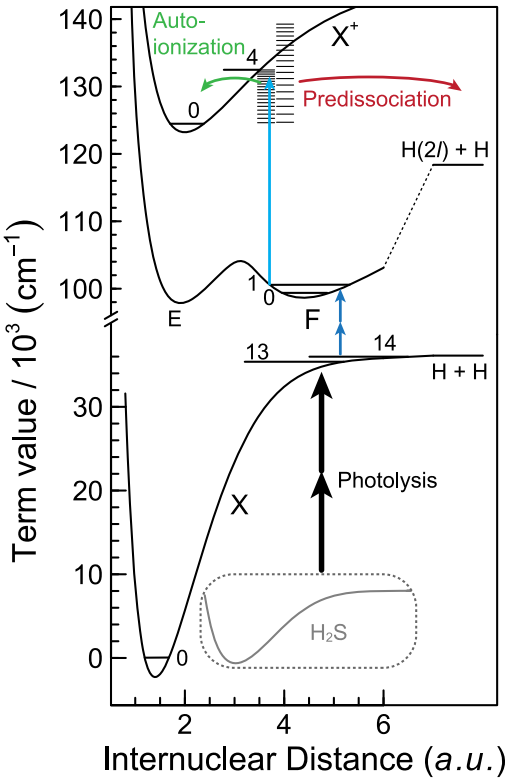

Figure 2. Excitation scheme followed in the present study. The highly excited H2 (v = 13, 14) states are produced by two photon UV-photolysis of H_2S. These states are subsequently interrogated via 2 + 1′ resonance-enhanced multiphoton ionization (three-laser scheme), while some overview spectra are recorded via via 2 + 1 REMPI (two-laser scheme). For further details, see text.

https://dx.doi.org/10.1021/acs.jpca.0c11136
J. Phys. Chem. A 2021, 125, 1221−1228

photolysis laser. For the same reason, the ionization laser is electronically delayed from the spectroscopy laser by 30 ns. H_2^+ ions produced are extracted into the mass-resolving time-of-flight tube and detected on an multichannel plate. The ion optics are triggered at about 50 ns delay from the ionization laser for avoiding dc-Stark fields during excitation.

III. RESULTS

First an overview spectrum was recorded using 2 + 1 REMPI on the $F^1\Sigma_g^+ - X^1\Sigma_g^+$ system in H_2 probing the population of high vibrational states in $X^1\Sigma_g^+$. This is done in a two-laser experiment, photolysis followed by one-color 2 + 1 REMPI, similar as in,[32] using both H_2^+ and H^+ detection. Here the resolution is limited by the bandwidth of the frequency-doubled pulsed dye laser (~0.1 cm^{-1}) used in the spectroscopy step. This overview spectrum, presented in Figure 3, displays

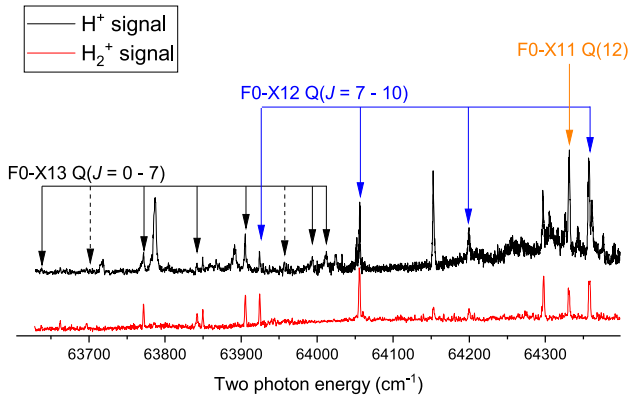

Figure 3. Low-resolution overview spectra of the $F^1\Sigma_g^+ - X^1\Sigma_g^+(0,13)$ and $F^1\Sigma_g^+ - X^1\Sigma_g^+(0,12)$ bands probed via one-color 2 + 1 REMPI with a tunable frequency-doubled pulsed dye laser upon H_2 photolysis. Signals are recorded for both H^+ and H_2^+.

rotational Q-lines in the F0-X12 and F0-X13 bands, along with some additional resonances, some of which could not be assigned. It is noted that the intensity of the lines is affected by the excitation step into the autoionization continuum via the resonant photon energy. The assignment of the F-X resonances derives from a comparison with combination differences between experimental level energies in $F^1\Sigma_g^+$ [39] and those of $X^1\Sigma_g^+$, obtained from the precise *ab initio* computations.[12]

Subsequently, precision measurements of the $F^1\Sigma_g^+ - X^1\Sigma_g^+$ electronic transitions are recorded under Doppler-free conditions, applying 2 + 1′ two-color REMPI in the three-laser scheme. While scanning the narrowband frequency-doubled PDA-system over the resonance, the third laser is set at a wavelength probing a strong as possible autoionization resonance, to be found in an iterative process. For these measurements H_2^+ ions are detected for registration of the spectra. Several Q-branch lines are measured probing $X^1\Sigma_g^+$, v = 13 levels (denoted as X13) in excitation to the lowest vibrational level (F0) in the $F^1\Sigma_g^+$ outer well for which the Franck–Condon factor is favorable.[40] All the odd J states of v = 13 are detected, where J = 7 is the highest bound state for v = 13 in H_2. Additionally, the Q(2) line in F0-X13 could be recorded, while the other even J states of para-hydrogen appeared to be too lowly populated to be detected in the high resolution measurement. Two of such spectra, for the Q(3) and Q(7) lines, are displayed in Figures 4 and 5.

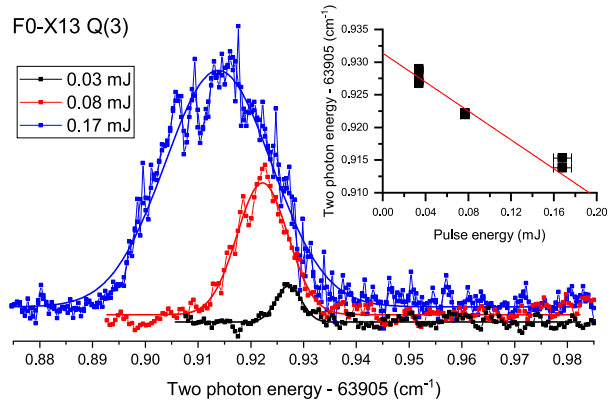

Figure 4. Spectra of the F0-X13 Q(3) transition recorded in a two-color 2 + 1′ REMPI scheme with tuning of the narrowband frequency-doubled PDA-system with counter-propagating UV-beams. The inset shows the ac-Stark extrapolation to zero power levels.

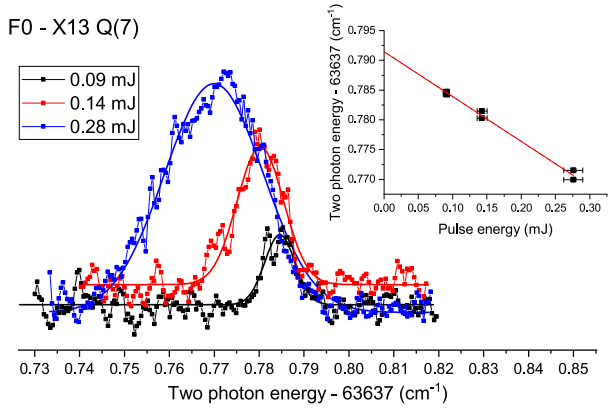

Figure 5. Spectra of the F0-X13 Q(7) transition; details as in Figure 4.

For the $X^1\Sigma_g^+$ v = 14 ground vibration, a high resolution recording could only be recorded for the J = 1 level at a low signal-to-noise ratio. Power-dependent spectral recordings are shown in Figure 6, where also an ac-Stark extrapolation curve is displayed. Excitation from other levels in v = 14 remained below the noise level.

The various sources of measurement uncertainty for the F1-X13 Q-branch lines, recorded in the three-laser scheme, are listed in Table 1. The major contribution to the total

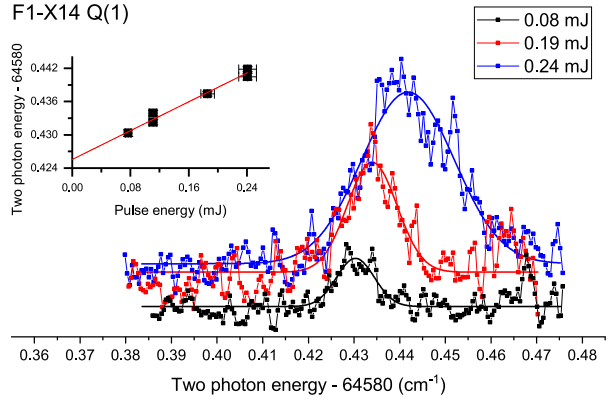

Figure 6. Spectra of the F1-X14 Q(1) transition; details as in Figure 4.

https://dx.doi.org/10.1021/acs.jpca.0c11136
J. Phys. Chem. A 2021, 125, 1221−1228

Table 1. Error Budget for the Two-Photon Frequencies for F0-X13 Q(J)

contribution	uncertainty ($\times 10^{-3}$ cm^{-1})
line profile (fitting)	0.5
statistics	2
ac-Stark extrapolation	1
frequency calibration	0.3
cw-pulse offset (chirp)	0.6
residual Doppler	<0.1
dc-Stark effect	<0.1
total	2.4

uncertainty is the statistical analysis over multiple sets of measurements, amounting to 2×10^{-3} cm^{-1}. The uncertainty in the frequency calibration of the cw-seed light, from the measurement of I_2-hyperfine lines and interpolation of FSR-markers of the reference etalon, contributes overall 3×10^{-4} cm^{-1} to the uncertainty. The chirp-induced frequency offset between the pulse generated from PDA system and the cw-seed light has been analyzed through established techniques,[38] adding 6×10^{-4} cm^{-1} to the frequency uncertainties. For the latter two contributions, a multiplication by a factor of 4 is included, for the frequency doubling and the two-photon process. The Doppler-free two-photon excitation with counter-propagating beams, enforced by the Sagnac interferometric alignment,[37] constrains the uncertainty from a residual Doppler effect below 1×10^{-4} cm^{-1}. Since the ion optics are triggered at least 80 ns delayed from the spectroscopy laser a dc-field-free environment is created, giving rise to a negligible dc-Stark effect to the accuracy.

The spectral recordings of the Doppler-free REMPI spectra undergo strong ac-Stark effects that contribute to the measurement uncertainty in two ways: asymmetric line profiles and shift of line center. The tightly focused PDA beams induce asymmetry of the line profile which limits the determination of line center. The spectra are fitted with Gaussian and skewed Gaussian profile to account for this line profile asymmetry. The uncertainty estimated from the extrapolation to zero-power yields 0.0005 cm^{-1}. For the low-power spectrum of the F0-X13 Q(3) line, with 0.03 mJ UV pulse energy, the line width is symmetric and about 180 MHz (fwhm), close to the expected instrumental line width determined by the laser bandwidth. For higher UV pulse energies, the spectral profiles become broadened and show a significant degree of asymmetry as result of spatial distribution of ac-Stark shifts in a tightly focused beam.[41] These lines are fitted with skewed Voigt profiles to determine the transition frequencies, as discussed previously.[33] The field-free transition frequencies are determined by extrapolation to zero power levels as shown in the insets of the figures.

The overall uncertainty results in 0.0024 cm^{-1}, corresponding to 70 MHz, by summing in quadrature for the F0-X13 Q-branch. For the F1-X14 Q(1) line 0.0040 cm^{-1} uncertainty is estimated, in view of the larger statistical uncertainty as a result of the poor signal-to-noise ratio obtained. Transition frequencies determined for the observed F0-X13 Q(J) and F1-X14 Q(1) lines, and the uncertainties, are listed in Table 2.

IV. DISCUSSION

The dissociation of H_2S in the present study is performed via two-photon absorption at 281.8 nm instead of 291.5 nm as was used in the previous studies,[33,34] where the highest level observed in H_2 ($X^1\Sigma_g^+$) was $v = 12, J = 5$. The energy required for complete dissociation of ground state H_2S into an $S(^1D_2)$ atom and two H atoms is about 69935(25) cm^{-1}.[36] The corresponding two-photon energy at 291.5 nm would reach only to about 1300 cm^{-1} below the H_2 dissociation limit, insufficient to produce H_2 fragments in $v = 13$ and $v = 14$. A 2 + 1 REMPI spectrum of H_2S shows a resonance at 281.8 nm, and when the dissociation laser wavelength was fixed to this resonance at 281.8 nm, the energetic region of 1000 cm^{-1} above the dissociation limit of H_2 can be probed and $v = 13$, 14 produced. The signal strength for odd-J transitions is generally stronger than for even-J transitions, reflecting the ortho-para distribution which is apparently maintained in the photolysis process. However, the signal intensity depends also on the efficiency of the autoionization induced by the setting of the third UV-laser.

In Table 2 a comparison is made between measured transition frequencies and predicted frequencies extracted from the calculated binding energies of $X^1\Sigma_g^+$ ($v = 13$) levels[12,13] and $F^1\Sigma_g^+$-state level energies obtained from Fourier transform (FT) spectroscopic measurements.[39] The uncertainty of the $X^1\Sigma_g^+$ state binding energies as obtained from the H2SPECTRE program suit[12] amounts nominally to 0.002−0.003 cm^{-1} with computed values listed in Table 2. For the experimentally determined level energies of F0, obtained up to $J = 5$ only, we have reanalyzed the uncertainties, based on the data presented in the Supporting Information of ref 39, because precision studies on the GK-X transition in H_2[42] have shown that some levels in ref.[39] exhibit a somewhat larger uncertainty than previously estimated. The reevaluated uncertainties are listed in Table 2. This comparison leads to fair agreement.

Table 2. Measured Frequencies for the Two-Photon F-X Transitions Probing the Highly Excited Vibrational Levels $X^1\Sigma_g^+$, v = 13, 14, with Uncertainties Indicated in Parentheses[a]

		expt	δF_{exp}	δX_{theo}	predicted	diff.
F0-X13	Q(1)	63 993.7920 (24)	0.004	0.0035	63 993.7956 (53)	−0.0036 (58)
	Q(2)	63 957.5160 (24)	0.002	0.0034	63 957.5236 (39)	−0.0076 (46)
	Q(3)	63 905.9305 (24)	0.010	0.0033	63 905.9369 (105)	−0.0064 (108)
	Q(5)	63 771.9836 (24)	0.015	0.0028	63 771.9723 (152)	+0.0113 (154)
	Q(7)	63 637.7937 (24)		0.0021		
F1-X14	Q(1)	64 580.4274 (40)	0.009	0.0017	64 580.4096 (92)	+0.0178 (95)

[a]These experimental values are compared with predicted values obtained via the combination of computed results for $X^1\Sigma_g^+$[12,13] and experimental values for $F^1\Sigma_g^+$.[39] The value for the F0 $J = 7$ level is absent in ref 39. The uncertainties in the experimental F-state level energies were reevaluated from the data reported in the Supporting Information of ref 39 and listed under δF_{exp}. Similarly the uncertainties in the calculated values of the X-levels, as determined from the H2SPECTRE program[12] are listed under δX_{theo}. All values in cm^{-1}.

https://dx.doi.org/10.1021/acs.jpca.0c11136
J. Phys. Chem. A 2021, 125, 1221−1228

Table 3. Combination Difference with Measured F0-X11 Transitions in Reference 33 and Comparison with Calculations in the Ground Electronic State[a]

	F0-X13	F0-X11	X13-X11	calculation	difference
Q(1)	63 993.7920 (24)	66 438.2920 (15)	2444.5000 (28)	2444.5019 (53)	−0.0019 (60)
Q(3)	63 905.9305 (24)	66 250.6874 (15)	2344.7569 (28)	2344.7489 (52)	+0.0080(59)
Q(5)	63 771.9836 (24)	65 931.3315 (15)	2159.3479 (28)	2159.3459 (51)	+0.0021(58)
Q(7)	63 637.7937 (24)	65 510.6124 (20)	1872.8187 (31)	1872.8277 (48)	−0.0090 (57)

[a]All values are presented in cm^{-1}, with uncertainties indicated in parentheses.

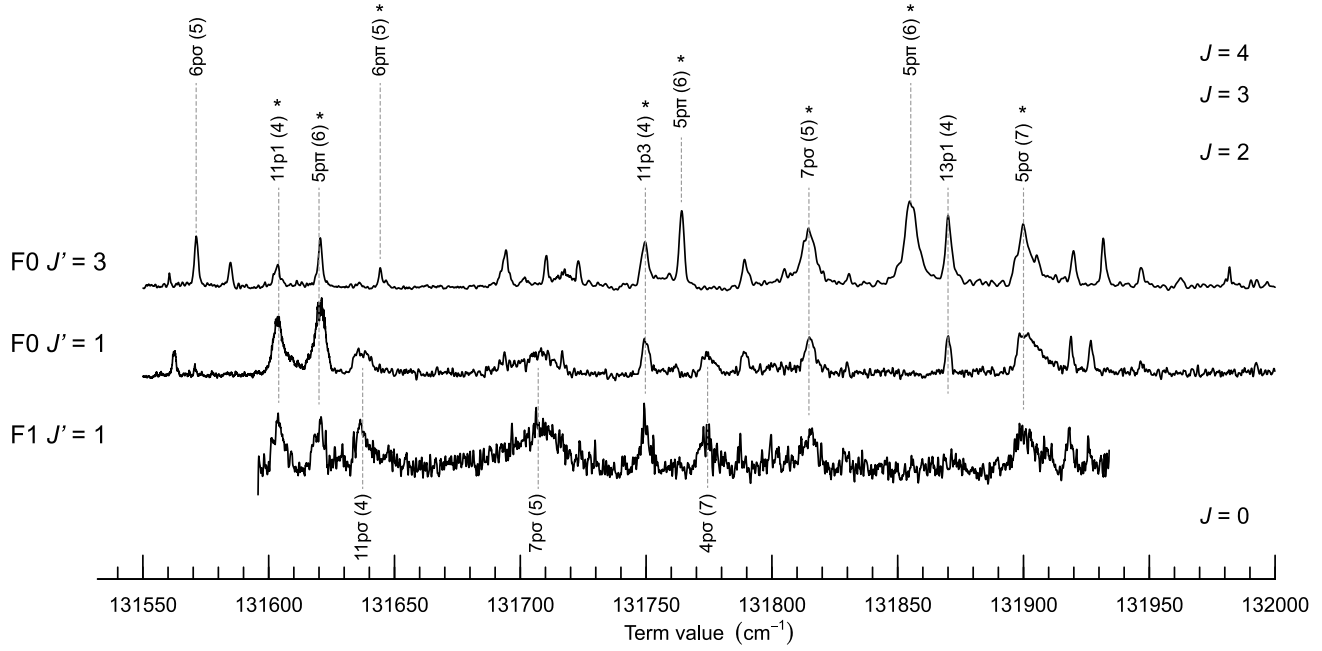

Figure 7. Autoionization spectra from F0 $J' = 1$, F1 $J' = 1$, and F0 $J' = 3$ intermediate levels. The horizontal axis reflects the total term value by adding the UV two-photon energy and the F-state level energy from ref 39: 99376.0474 cm^{-1} for F0 $J = 1$, 100570.843 cm^{-1} for F1 $J = 1$, and 99437.1665 cm^{-1} for F0 $J = 3$. The resonances in the autoionization continuum are labeled in either Hund's case (b) $np\lambda(v^+)$ or (d) $npN^+(v^+)$, where v^+ and N^+ are the vibrational and the rotational quantum numbers of the H_2^+ ion core. The total angular momentum quantum number J of the H_2 continuum resonance is given on the right. Previously observed resonances[43−45] are indicated by an asterisk.

In order to test the full QED-relativistic calculations of the ground state binding energies, a further comparison is made using combination differences from experiment, independent of data on F-level energies from ref.[39] The previous experimental values on F0-X11 Q-transitions[33] are subtracted from the present values for F0-X13 Q-transitions to obtain vibrational splittings between X13 and X11 levels which can be compared with the same combination differences from the most advanced first-principles calculations.[12,13] Table 3 presents these comparisons for four sets of J-levels. The experimentally derived splittings between $v = 11$ and $v = 13$ agree with the calculations at a root-mean-square value of $\pm 1.07\sigma$.

These result provide a test on the accuracy of the ab initio computations for ground state levels, for the first time for the highest v-levels in the $X^1\Sigma_g^+$ ground state of H_2. The current theoretical values are limited by nonadiabatic contributions to the relativistic energy.[13] Meanwhile, improved fully variational calculations have been developed, that led to an uncertainty less than 10^{-7} cm^{-1}, but as of yet only for the $X^1\Sigma_g^+$ ($v = 0$, $J = 0$) ground state.[11]

As for the F1-X14 Q(1) line no such comparison could be made, because the F1-X13 and F1-X12 Q(1) transitions appeared too weak in the high precision measurement. In the search of $v = 14$ in H_2, excitations to F0, F1 and F2 states were tested but only a single F1-X14 Q(1) line is confirmed. The absence of F0-X14 lines could be explained by the small Franck−Condon factor, which is about 70-times smaller than that for F1-X14.[40] The assignment of F1-X14 Q(1) is verified by comparing autoionization spectra recorded in the region below the $X^+(v^+ = 4, J^+ = 1)$ ionization threshold as shown in Figure 7. The F-outer-well state has nominally $(2p\sigma_u)^2$ character and we observe exclusively transitions to vibrationally autoionizing $(1s\sigma)(np\sigma/\pi)$ Rydberg states, with n being the principal quantum number. To guide the assignment we carried out multichannel quantum-defect (MQDT) calculations as described in ref 46 using the quantum-defect functions derived in ref.[47] We note that states with Σ^+ and Π^+ symmetry are subject to predissociation into the H + H($n = 2$) continuum, leading to broad resonances especially for low n-values. The interaction with the dissociation continuum was not included in our calculation, leading to deviations of the calculated term values for the low-n resonances on the order of 1 cm^{-1}. The experimental line positions for these states are however in good agreement with previously reported values and MQDT calculations including the combined ionization and dissociation continuum.[43−45]

Autoionization spectra are recorded by fixing the PDA-spectroscopy laser on two-photon resonances probing F0 $J = 1$, F0 $J = 3$ and F1 $J = 1$, and are plotted on an energy scale

https://dx.doi.org/10.1021/acs.jpca.0c11136
J. Phys. Chem. A 2021, 125, 1221−1228

relative to the X, $v = 0$, $J = 0$ state of H_2. The fact that the autoionization spectrum from F0 $J = 1$, probed via X13 $J = 1$, exhibits the same resonances as the autoionization spectrum from F1 $J = 1$, probed via X14 $J = 1$, proves that the two-photon resonance at 64 580.427 cm^{-1} starts from a $J = 1$ line, which leads to an unambiguous assignment of the F1-X14 Q(1) transition. Unfortunately no other rotational levels in X14 could be found. There appears a strong transition at 64563.084 cm^{-1}, while the expected F1-X14 Q(3) is at 64562.883 cm^{-1}, exhibiting a 0.201 cm^{-1} difference. Also in this case an autoionization spectrum is recorded from this intermediate state, but that does not match with an autoionization spectrum from F0 $J = 3$. Hence the assignment of the F1-X14 Q(3) line is discarded.

As a byproduct of the present study the Stark slopes of the two-photon transitions are determined, results of which are shown in the insets of Figures 4−6. Those represent the shift of line center as a result of the ac-Stark effect, i.e., the power density; a negative Stark slope corresponds to a red-shift of the lines for higher power densities. Stark slopes for the F0-X13 band are all negative, while that of the single transition in the F1-X14 band is found positive. In a previous study a negative Stark slope was found for lines in the F0-X11 band, where a very small J-dependent value was found for the F3-X12 band.[33] Similarly, in two-photon excitation to the inner well positive Stark slopes were found for the E0-X0 band[48] and the E0-X1 band.[49] These Stark slopes depend on the transition dipole moments in summation over all states in the molecule[50,51] thus providing information on the quantum structure of the molecule, analysis of which is beyond the scope of this study.

V. CONCLUSION

In the present study two-photon UV-photolysis of H_2S was pursued, probing a two-photon absorption resonance at 281.8 nm, hence at sufficiently short wavelength to produce H_2 molecules in the highest vibrational levels: $v = 13$, 14. The transition energies of F-X (0,13) Q-branch lines have been measured at an accuracy of 0.0024 cm^{-1}. In comparing these results with previous measurements on F0-X11 Q-lines the experimental combination difference can be used to verify level splittings as computed with advanced quantum chemical calculations of the ground electronic state of H_2, including nonadiabatic, relativistic and QED effects. This results in good agreement. Also the highest vibrational state $v = 14$ of H_2 has been produced through the two-photon photodissociation of H_2S. Only a single rotational level $J = 1$ could be observed. The assignment of this $X^1\Sigma_g^+$ ($v = 14$, $J = 1$) level was verified by recording and comparing autoionization spectra from various F-outer well states.

The total uncertainty in the present study is limited by measurement statistics, associated with the low concentration of H_2 fragments produced, and by strong ac-Stark effects resulting from the focused UV-laser beams required to obtain signal. Further improvement of the H_2S photolysis production process is critical for pursuing higher measurement accuracy. Under such improved conditions the entire rotational manifold $J = 0$−3 of bound levels in $v = 14$ might be probed and studied and implemented in QED-test of such weakly bound states at large internuclear separation. It has been a matter of debate whether the final level $J = 4$ is rotationally predissociative,[52] only bound by nonadiabatic effects,[53] or quasi-bound due to hyperfine effects.[54] As an outlook it may be hypothesized that also quasi-bound states in H_2 might be observed by the methods pursued here.

AUTHOR INFORMATION

Corresponding Author

W. Ubachs − *Department of Physics and Astronomy, LaserLaB, Vrije Universiteit, 1081 HV Amsterdam, The Netherlands*; orcid.org/0000-0001-7840-3756; Email: w.m.g.ubachs@vu.nl

Authors

K.-F. Lai − *Department of Physics and Astronomy, LaserLaB, Vrije Universiteit, 1081 HV Amsterdam, The Netherlands*

M. Beyer − *Department of Physics and Astronomy, LaserLaB, Vrije Universiteit, 1081 HV Amsterdam, The Netherlands*

E. J. Salumbides − *Department of Physics and Astronomy, LaserLaB, Vrije Universiteit, 1081 HV Amsterdam, The Netherlands*

Complete contact information is available at: https://pubs.acs.org/10.1021/acs.jpca.0c11136

Notes

The authors declare no competing financial interest.

ACKNOWLEDGMENTS

The authors thank Dr. Christian Jungen for fruitful discussions and for making available his MQDT-codes for calculating and assigning the autoionization resonances. W.U. acknowledges the European Research Council for an ERC Advanced Grant (No. 670168).

REFERENCES

(1) Lyman, T. The Spectrum of Hydrogen in the Region of Extremely Short Wavelengths. *Astrophys. J.* **1906**, *23*, 181.

(2) Herzberg, G.; Howe, L. L. The Lyman bands of molecular hydrogen. *Can. J. Phys.* **1959**, *37*, 636.

(3) Herzberg, G.; Jungen, C. Rydberg series and ionization potential of the H_2 molecule. *J. Mol. Spectrosc.* **1972**, *41*, 425.

(4) Chupka, W. A. Photoionization of molecular Rydberg states: H_2, $C^1\Pi_u$ and its doubly excited states. *J. Chem. Phys.* **1987**, *87*, 1488.

(5) Herzberg, G. Quadrupole rotation-vibration spectrum of the hydrogen molecule. *Nature* **1949**, *163*, 170.

(6) James, H. M.; Coolidge, A. S. The Ground State of the Hydrogen Molecule. *J. Chem. Phys.* **1933**, *1*, 825.

(7) Kołos, W.; Wolniewicz, L. Improved Theoretical Ground-State Energy of the Hydrogen Molecule. *J. Chem. Phys.* **1968**, *49*, 404.

(8) Wolniewicz, L. Nonadiabatic energies of the ground state of the hydrogen molecule. *J. Chem. Phys.* **1995**, *103*, 1792.

(9) Dressler, K.; Wolniewicz, L. Improved adiabatic corrections for the $B^1\Sigma_u^+$, $C^1\Pi_u$, and $D^1\Pi_u$ states of the hydrogen molecule and vibrational structures for H_2, HD, and D_2. *J. Chem. Phys.* **1986**, *85*, 2821.

(10) Komasa, J.; Piszczatowski, K.; Łach, G.; Przybytek, M.; Jeziorski, B.; Pachucki, K. Quantum Electrodynamics Effects in Rovibrational Spectra of Molecular Hydrogen. *J. Chem. Theory Comput.* **2011**, *7*, 3105.

(11) Komasa, J.; Puchalski, M.; Czachorowski, P.; Lach, G.; Pachucki, K. Rovibrational energy levels of the hydrogen molecule through nonadiabatic perturbation theory. *Phys. Rev. A: At., Mol., Opt. Phys.* **2019**, *100*, No. 032519.

(12) *H2SPECTRE ver 7.0 Fortran source code*; University of Warsaw: Warsaw, Poland, 2019.

(13) Czachorowski, P.; Puchalski, M.; Komasa, J.; Pachucki, K. Nonadiabatic relativistic correction in H_2, D_2, and HD. *Phys. Rev. A: At., Mol., Opt. Phys.* **2018**, *98*, No. 052506.

(14) Marinero, E. E.; Vasudev, R.; Zare, R. N. The E,F $^1\Sigma_g^+$ double-minimum state of hydrogen: Two-photon excitation of inner and outer wells. *J. Chem. Phys.* **1983**, *78*, 692.
(15) Dickenson, G. D.; Salumbides, E. J.; Niu, M.; Jungen, C.; Ross, S. C.; Ubachs, W. Precision spectroscopy of high rotational states in H_2 investigated by Doppler-free two-photon laser spectroscopy in the $EF^1\Sigma_g^+ - X^1\Sigma_g^+$ system. *Phys. Rev. A: At., Mol., Opt. Phys.* **2012**, *86*, No. 032502.
(16) Wolniewicz, L.; Dressler, K. The EF, GK, and $H\bar{H}^1\Sigma_g^+$ states of hydrogen. Improved ab initio calculation of vibrational states in the adiabatic approximation. *J. Chem. Phys.* **1985**, *82*, 3292.
(17) Reinhold, E.; Hogervorst, W.; Ubachs, W. Observation of a Highly Excited Long-Lived Valence State in H_2. *Phys. Rev. Lett.* **1997**, *78*, 2543.
(18) Yu, S.; Dressler, K. Calculation of rovibronic structures in the lowest nine excited $^1\Sigma_g^+ + {}^1\Pi_g + {}^1\Delta_g$ states of H_2, D_2, and T_2. *J. Chem. Phys.* **1994**, *101*, 7692.
(19) Reinhold, E.; de Lange, A.; Hogervorst, W.; Ubachs, W. Observation of the $I'^1\Pi_g$ outer well state in H_2 and D_2. *J. Chem. Phys.* **1998**, *109*, 9772.
(20) Kołos, W. Ab initio potential energy curves and vibrational levels for the B″ and B′ states of the hydrogen molecule. *J. Mol. Spectrosc.* **1976**, *62*, 429.
(21) de Lange, A.; Hogervorst, W.; Ubachs, W.; Wolniewicz, L. Double-Well States of Ungerade Symmetry in H_2: First Observation and Comparison with Ab Initio Calculations. *Phys. Rev. Lett.* **2001**, *86*, 2988.
(22) Reinhold, E.; Ubachs, W. Heavy Rydberg states. *Mol. Phys.* **2005**, *103*, 1329.
(23) Beyer, M.; Merkt, F. Observation and Calculation of the Quasibound Rovibrational Levels of the Electronic Ground State of H_2^+. *Phys. Rev. Lett.* **2016**, *116*, No. 093001.
(24) Beyer, M.; Merkt, F. Half-Collision Approach to Cold Chemistry: Shape Resonances, Elastic Scattering, and Radiative Association in the $H^+ + H$ and $D^+ + D$ Collision Systems. *Phys. Rev. X* **2018**, *8*, No. 031085.
(25) Aker, P. M.; Germann, G. J.; Valentini, J. J. State-to-state dynamics of H+HX collisions. I. The H+HX → H_2+X (X = Cl,Br,I) abstraction reactions at 1.6 eV collision energy. *J. Chem. Phys.* **1989**, *90*, 4795.
(26) Kliner, D.; Rinnen, K.; Buntine, M.; Adelman, D.; Zare, R. N. Product internal-state distribution for the reaction H + HI → H_2+I. *J. Chem. Phys.* **1991**, *95*, 1663.
(27) Robie, D.; Jusinski, L.; Bischel, W. Generation of highly vibrationally excited H_2 and detection by 2 + 1 resonantly enhanced multiphoton ionization. *Appl. Phys. Lett.* **1990**, *56*, 722.
(28) Pomerantz, A.; Ausfelder, F.; Zare, R. N.; Huo, W. Line strength factors for $E,F^1\Sigma_g^+(v' = 0,J' = J'')$-$X^1\Sigma_g^+(v'',J'')$ (2 + 1) REMPI transitions in molecular hydrogen. *Can. J. Chem.* **2004**, *82*, 723.
(29) Mukherjee, N.; Perreault, W. E.; Zare, R. N. Stark-induced adiabatic Raman ladder for preparing highly vibrationally excited quantum states of molecular hydrogen. *J. Phys. B: At., Mol. Opt. Phys.* **2017**, *50*, 144005.
(30) Perreault, W. E.; Zhou, H.; Mukherjee, N.; Zare, R. N. Harnessing the Power of Adiabatic Curve Crossing to Populate the Highly Vibrationally Excited H_2 (v = 7, j = 0) Level. *Phys. Rev. Lett.* **2020**, *124*, 163202.
(31) Steadman, J.; Baer, T. The production and characterization by resonance enhanced multiphoton ionization of H_2 (v = 10 − 14) from photodissociation of H_2S. *J. Chem. Phys.* **1989**, *91*, 6113.
(32) Niu, M. L.; Salumbides, E. J.; Ubachs, W. Communication: Test of quantum chemistry in vibrationally hot hydrogen molecules. *J. Chem. Phys.* **2015**, *143*, No. 081102.
(33) Trivikram, T. M.; Niu, M. L.; Wcisło, P.; Ubachs, W.; Salumbides, E. J. Precision measurements and test of molecular theory in highly excited vibrational states of H_2 (v = 11). *Appl. Phys. B: Lasers Opt.* **2016**, *122*, 294.
(34) Trivikram, T. M.; Salumbides, E. J.; Jungen, C.; Ubachs, W. Excitation of H_2 at large internuclear separation: outer well states and continuum resonances. *Mol. Phys.* **2019**, *117*, 2961.
(35) Quinn, M. S.; Nauta, K.; Kable, S. H. Disentangling the H_2 $EF(^1\Sigma_g^+)$ (v = 0 − 18) - X $(^1\Sigma_g^+)$ (v = 3 − 9) (2 + 1) REMPI spectrum via 2D velocity-mapped imaging. *Mol. Phys.* **2021**, *119*, No. e1836412.
(36) Zhou, J.; Zhao, Y.; Hansen, C. S.; Yang, J.; Chang, Y.; Yu, Y.; Cheng, G.; Chen, Z.; He, Z.; Yu, S.; Ding, H.; Zhang, W.; Wu, G.; Dai, D.; Western, C. M.; Ashfold, M. N.; Yuan, K.; Yang, X. Ultraviolet photolysis of H_2S and its implications for SH radical production in the interstellar medium. *Nat. Commun.* **2020**, *11*, 1547.
(37) Hannemann, S.; Salumbides, E. J.; Ubachs, W. Reducing the first-order Doppler shift in a Sagnac interferometer. *Opt. Lett.* **2007**, *32*, 1381.
(38) Eikema, K. S. E.; Ubachs, W.; Vassen, W.; Hogervorst, W. Lamb shift measurement in the 1 ^{1}S ground state of helium. *Phys. Rev. A: At., Mol., Opt. Phys.* **1997**, *55*, 1866.
(39) Bailly, D.; Salumbides, E.; Vervloet, M.; Ubachs, W. Accurate level energies in the $EF^1\Sigma_g^+$, $GK^1\Sigma_g^+$, $H^1\Sigma_g^+$, $B^1\Sigma_u^+$, $C^1\Pi_u$, $B'^1\Sigma_u^+$, $D^1\Pi_u$, $I^1\Pi_g$, $J^1\Delta_g$ states of H_2. *Mol. Phys.* **2010**, *108*, 827.
(40) Fantz, U.; Wünderlich, D. Franck−Condon factors, transition probabilities, and radiative lifetimes for hydrogen molecules and their isotopomeres. *At. Data Nucl. Data Tables* **2006**, *92*, 853.
(41) Li, L.; Yang, B.-X.; Johnson, P. M. Alternating-current Stark-effect line shapes in multiphoton ionization spectra. *J. Opt. Soc. Am. B* **1985**, *2*, 748.
(42) Cheng, C.-F.; Hussels, J.; Niu, M.; Bethlem, H. L.; Eikema, K. S. E.; Salumbides, E. J.; Ubachs, W.; Beyer, M.; Hölsch, N.; Agner, J. A.; Merkt, F.; Tao, L.-G.; Hu, S.-M.; Jungen, C. Dissociation Energy of the Hydrogen Molecule at 10^{-9} Accuracy. *Phys. Rev. Lett.* **2018**, *121*, No. 013001.
(43) Glass-Maujean, M.; Jungen, C.; Spielfiedel, A.; Schmoranzer, H.; Tulin, I.; Knie, A.; Reiss, P.; Ehresmann, A. Experimental and theoretical studies of excited states of H_2 observed in the absorption spectrum: I. The 5pπ D″ $^1\Pi_u$ state. *J. Mol. Spectrosc.* **2013**, *293-294*, 1.
(44) Glass-Maujean, M.; Jungen, C.; Schmoranzer, H.; Tulin, I.; Knie, A.; Reiss, P.; Ehresmann, A. Experimental and theoretical studies of excited states of H_2 observed in the absorption spectrum: II. The 6pπ and 7pπ $^1\Pi_u$ states. *J. Mol. Spectrosc.* **2013**, *293-294*, 11.
(45) Glass-Maujean, M.; Jungen, C.; Schmoranzer, H.; Tulin, I.; Knie, A.; Reiss, P.; Ehresmann, A. Experimental and theoretical studies of excited states of H_2 observed in the absorption spectrum: III. The 5pσ, 6pσ and 7pσ states. *J. Mol. Spectrosc.* **2013**, *293-294*, 19.
(46) Jungen, C.; Atabek, O. Rovibronic interactions in the photoabsorption spectrum of molecular hydrogen and deuterium: An application of multichannel quantum defect methods. *J. Chem. Phys.* **1977**, *66*, 5584.
(47) Sprecher, D.; Jungen, C.; Merkt, F. Determination of the binding energies of the *np* Rydberg states of H_2, HD, and D_2 from high-resolution spectroscopic data by Multichannel Quantum-Defect Theory. *J. Chem. Phys.* **2014**, *140*, 104303.
(48) Hannemann, S.; Salumbides, E. J.; Witte, S.; Zinkstok, R. T.; van Duijn, E. J.; Eikema, K. S. E.; Ubachs, W. Frequency metrology on the $EF^1\Sigma_g^+ - X^1\Sigma_g^+$ (0,0) transition in H_2, HD, and D_2. *Phys. Rev. A: At., Mol., Opt. Phys.* **2006**, *74*, No. 062514.
(49) Niu, M. L.; Salumbides, E. J.; Dickenson, G. D.; Eikema, K. S. E.; Ubachs, W. Precision spectroscopy of the $X^1\Sigma_g^+$, $v = 0 \rightarrow 1$ ($J = 0 - 2$) rovibrational splittings in H_2, HD and D_2. *J. Mol. Spectrosc.* **2014**, *300*, 44.
(50) Girard, B.; Billy, N.; Vigue, J.; Lehmann, J. Evidence for a dynamical stark effect in CO ($A^1\Pi$) two-photon excitation. *Chem. Phys. Lett.* **1983**, *102*, 168.
(51) Huo, W. M.; Gross, K. P.; McKenzie, R. L. Optical Stark Effect in the Two-Photon Spectrum of NO. *Phys. Rev. Lett.* **1985**, *54*, 1012.
(52) Le Roy, R. J.; Bernstein, R. B. Shape Resonances and Rotationally Predissociating Levels: The Atomic Collision Time-Delay Functions and Quasibound Level Properties of H_2 ($X^1\Sigma_g^+$). *J. Chem. Phys.* **1971**, *54*, 5114.

https://dx.doi.org/10.1021/acs.jpca.0c11136
J. Phys. Chem. A 2021, 125, 1221−1228

(53) Pachucki, K.; Komasa, J. Nonadiabatic corrections to rovibrational levels of H_2. *J. Chem. Phys.* **2009**, *130*, 164113.
(54) Selg, M. A quasi-bound rovibrational state of hydrogen molecule resulting from hyperfine proton-electron spin-spin interaction. *Eur. Phys. Lett.* **2011**, *96*, 10009.

https://dx.doi.org/10.1021/acs.jpca.0c11136
J. Phys. Chem. A 2021, 125, 1221−1228